

# Implications of Modelled Climate and Land Cover Changes on Runoff in the Middle Route of the South to North Water Transfer Project in China

Lingcheng Li · Liping Zhang · Jun Xia ·  
Christopher James Gippel · Renchao Wang ·  
Sidong Zeng

Received: 24 June 2014 / Accepted: 16 February 2015 /  
Published online: 10 March 2015  
© Springer Science+Business Media Dordrecht 2015

**Abstract** Sustainable management of water for human uses and maintaining river health requires reliable information about the future availability of water resources. We quantified the separate and combined impacts of climate and land cover changes on runoff for the historical record and for modelled future scenarios in the upper Han River and Luan River, supply and demand zones respectively of the middle route of the South to North Water Transfer Project in China, the world's largest inter-basin water transfer project. We used a precipitation-runoff model, averaged multiple climate model predictions combined with three emissions scenarios, a combined CA-Markov model to predict land cover change, and a range of statistical tests. Comparing baseline with 2050: climate change would cause an average reduction in runoff of up to 15 % in the upper Han River and up to 9 % in the Luan River catchment; a scenario involving increased forest cover would reduce runoff by up to 0.19 % in the upper Han River and up to 35 % in the Luan River; a scenario involving increased grass cover would increase runoff by up to 0.42 % in the upper Han River and up to 20 % in the Luan River. In the lower Luan River, the mean annual flow after 1998 fell to only 17 % of that of the baseline period, posing a serious threat to river health. This was explained largely by extraction of surface water and groundwater, rather than climate and land use change.

---

L. Li · L. Zhang (✉) · J. Xia · R. Wang · S. Zeng  
State Key Laboratory of Water Resources and Hydropower Engineering Science, Wuhan University,  
Wuhan 430072, People's Republic of China  
e-mail: zhanglp@whu.edu.cn

L. Zhang  
College of Tourism Culture and Geographical Science, Huanggang Normal University, Huanggang 438000,  
People's Republic of China

L. Li · J. Xia · S. Zeng  
Hubei Collaborative Innovation Center for Water Resources Security, Wuhan University, Wuhan 430072,  
People's Republic of China

C. J. Gippel  
Australian Rivers Institute, Griffith University, Nathan, Queensland 4111, Australia

**Keywords** Runoff change · Climate change · Land cover change · SWAT model · CA-Markov model · Water transfer

## 1 Introduction

The main factors that drive change in the temporal and spatial distribution of runoff are climate and land cover changes (Shi et al. 2013), and direct alteration by flow regulation, diversion and groundwater pumping. Understanding these processes can make an important contribution to the development of socially, economically and ecologically sustainable water resources management strategies (Cao et al. 2009; Narsimlu et al. 2013). Large cities in northern China have been under water stress since the 1980s, alleviated only through a number of temporary solutions (Peisert and Sternfeld 2005; Xia et al. 2007). The South to North Water Transfer Project (SNWTP), the world's largest inter-basin water transfer project in the world's most populous region, was conceived as a long-term solution to the geographical imbalance in water availability in China. Launched in 2002, it will ultimately transfer  $44.8 \times 10^9 \text{ m}^3$  per year from the wetter regions of southern China via three routes, the western, eastern and central routes, to the drier northern regions. The middle route, set for completion in 2014, will provide  $13 \times 10^9 \text{ m}^3$  per year from the Danjiangkou Reservoir on the Han River, the biggest tributary of the Yangtze River, to Beijing and Tianjin, the two largest cities in northern China. Berkoff (2003) and Yang and Zehnder (2005) recognised that rehabilitation of aquatic ecosystem health in the highly degraded northern rivers of China was one of the strongest arguments in favour of the SNWTP. The effectiveness of the operation of the middle route of the SNWTP in achieving its social and ecological objectives fundamentally depends on the future pattern of natural runoff and water utilization in the catchments of Danjiangkou Reservoir (the supply zone) and the Hai River basin (the demand zone).

While a number of previous studies have investigated the hydrology of the Han River Basin (e.g., Zhang et al. 2012) and Hai River Basin (Yang and Tian 2009) using various methods, this paper allows direct comparison of the hydrology of the supply and demand zones of the SNWTP. The main argument presented here is that the potential impact of climate and land cover change on runoff is great enough that it warrants careful consideration in the planning and management of major water resources development projects like the SNWTP. We demonstrate this point by quantifying the impacts of climate and land cover changes on runoff, for the historical record and for modelled future climate and land cover change scenarios, in the upper Han River and the Luan River (considered part of the Hai River basin), and then compare these impacts with direct human impacts on river flows. We consider the broad consequences of the observed and predicted future runoff changes for river health.

## 2 Study Areas

The upper Han River catchment is situated between  $31.4\text{--}34.1^\circ\text{N}$  and  $106\text{--}112^\circ\text{E}$ , with an elevation from 210 m to 3 549 m (Fig. 1) and a drainage area of  $94\,173 \text{ km}^2$  at Danjiangkou Reservoir. The Danjiangkou dam was constructed between 1958 and 1973 with a capacity of  $17.45 \times 10^9 \text{ m}^3$ , and enlarged between 2005 and 2009 to  $29.05 \times 10^9 \text{ m}^3$ . Over the period 1961–2008 the mean annual catchment temperature was  $14.6^\circ\text{C}$ , mean annual catchment precipitation was 821 mm, and the mean annual runoff was 396 mm. About 80 % of the annual precipitation falls from May to October.

The Luan River catchment is located between  $39.1\text{--}42.5^\circ\text{N}$  and  $115.5\text{--}119.3^\circ\text{E}$ , with an elevation from sea level to 2210 m (Fig. 1) and a drainage area of  $44\,697 \text{ km}^2$ . The Panjiakou-

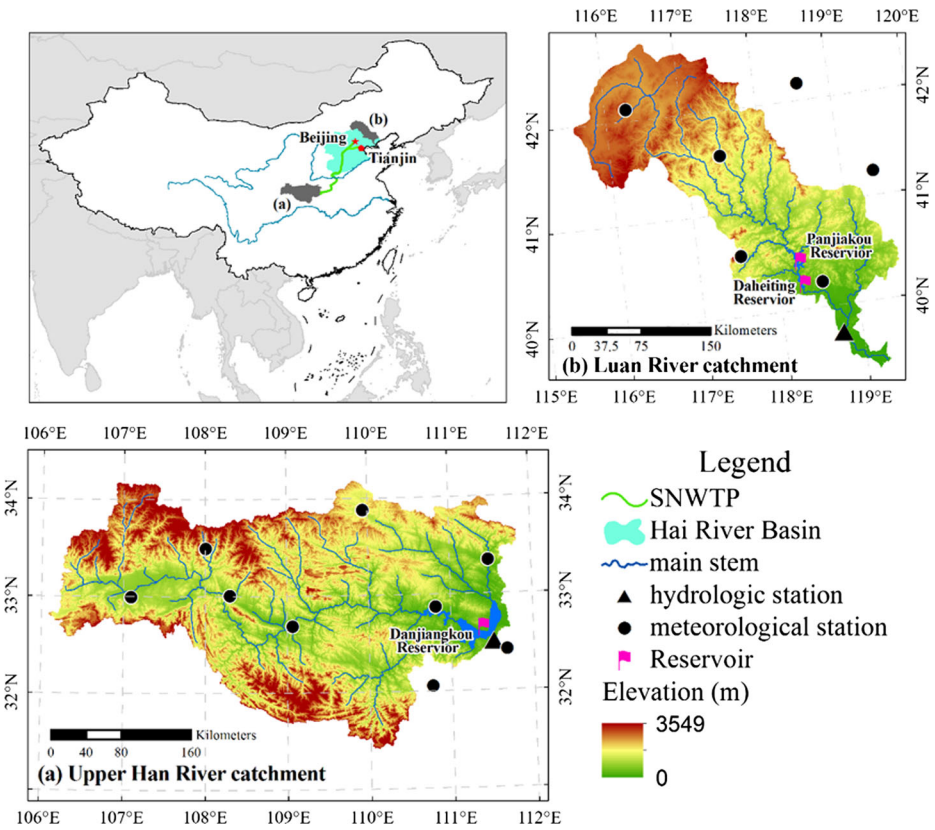


**Fig. 1** Location of the upper Han River and Luan River catchments. Some of the marked islands in the South China Sea are disputed territory

Daheting Reservoir system, which began operation in 1981, has a catchment area of 33 700 km<sup>2</sup> (about 75 % of the total catchment area). The construction of a diversion from the Panjiakou-Daheting Reservoir system to Tianjin City was built in 1983. Another project built in 1984 diverts water to Tangshan City, and another smaller project built in 1989 diverts water from the Taolinkou Reservoir to Qinhuangdao and Lulong. Over the period 1960–2010 the mean annual catchment temperature was 7.0 °C and the mean annual catchment precipitation was 473 mm. About 70 % of the precipitation falls from July to September.

### 3 Data and Methods

#### 3.1 Datasets

Daily meteorological data were obtained from the China Meteorological Data Sharing Service System for nine meteorological stations in Han River catchment and six meteorological stations in Luan River catchment (Fig. 1). The Thiessen polygon method was used to generate a single catchment annual precipitation series. An annual potential evapotranspiration series for each catchment was generated from the climate data by the Penman-Monteith equation. Monthly runoff data for river gauging stations located at the downstream end of each catchment were

supplied by the Changjiang Water Resources Commission (CWRC) and Haihe Water Resources Commission. Upper Han River runoff data were based on data from Huangjiagang gauge, located just downstream of Danjiangkou reservoir, for the period 1961–2008. The supplied data were reconstructed by the CWRC to simulate reservoir inflows, thus representing flows unimpacted by operation of the dam. Luan River runoff data were from the Luanxian gauge for the period 1960–2010. The Luanxian gauge is located downstream of the Panjiakou-Daheting Reservoir system and the Tianjin, Tangshan and Qinhuangdao flow diversions (Fig. 1). Estimated annual inflows to Panjiakou-Daheting Reservoir system over the period 1960–2003 were taken from Hao (2007), supplemented with data over the period 2004–2009 from Wang (2011). Data on annual water diversions from Panjiakou-Daheting Reservoir system to Tianjin over the period 1987–1999 were taken from Zhang et al. (2008), supplemented with data over the period 2000–2010 from Tianjin Water Supply Bureau (2000–2010).

GTOPO30 digital elevation models (DEM) at 30-arc sec resolution (approximately 1 km), were obtained from the US Geological Survey. Soil type and land cover data at 1 km resolution were obtained for 1980, 1990 and 2000 from the Data Center for Resources and Environmental Sciences, Chinese Academy of Sciences. We reclassified the land cover data according to the land cover categories available in SWAT.

### 3.2 Precipitation-Runoff Model

We used the SWAT model (Gassman et al. 2007) to predict runoff, employing the modified Soil Conservation Service curve number method for surface runoff calculation, the Penman-Monteith equation to estimate potential evapotranspiration, and the Muskingum procedure for flow routing. The SWAT model was calibrated and validated using data from the baseline part of the historical runoff series, identified through step change analysis. Here, the term ‘baseline’ means unimpacted by land cover change, climate change, regulation or other major human disturbances. The baseline period was divided into two parts, one for calibration and the other for validation. For the upper Han River catchment, the calibration period was 1961–1978 and the validation period was 1979–1985, while for the Luan River catchment the calibration period was 1960–1972 and the validation period was 1973–1979.

SUFI-2 (Sequential Uncertainty Fitting, ver. 2) (Abbaspour 2007) was used for a combined calibration and uncertainty analysis, linked to SWAT in the calibration package SWAT-CUP. This approach has been used for calibration and quantification of uncertainty in large and small watersheds (e.g., Al-Mukhtar et al. 2014). The overall prediction uncertainty was quantified by the 95 % prediction uncertainty (95PPU), calculated at the 2.5 and 97.5 % levels of the cumulative distribution of an output variable obtained through Latin hypercube sampling. Calibration was undertaken with the objective of achieving the closest fit between modelled and observed data, as measured by Nash–Sutcliffe efficiency (NSE), correlation coefficient (R) and relative bias (BIAS). We also used these tests to measure the performance of the model in the validation period.

### 3.3 Tests for Non-stationarity in Runoff and Climate Time Series

Non-stationarity in runoff and climate data series was investigated using the procedures outlined by Chiew and McMahon (1993). Trend was tested using the Mann-Kendall (MK) test ( $z$  statistic), and step change was identified using the Cumulative deviation (CD) test ( $Q/\sqrt{n}$  statistic), the Worsley likelihood ratio (WLR) test ( $W$  statistic) and the distribution-free CUSUM test ( $\max |V_k|$  statistic). TREND software (Chiew and Siriwardena 2005) was used to perform the statistical tests, and we additionally used Sen’s slope method (Sen 1968) to

estimate the slope of trend based on Kendall's tau. For all tests, a minimum threshold of  $\alpha=0.05$  was used to test for significance. We used these tests to divide the upper Han and Luan river runoff series into two periods, with the earlier period termed 'baseline' and the post-change point period termed 'impacted'. The future scenario series were also regarded as impacted, because compared with the baseline period, major climate and land cover changes were imposed to create these scenarios. To compare two series created by a change point, or to compare a historical and modelled series, we used the Student's *t* test for difference in means.

### 3.4 Climate Change Scenarios

As is common practice when using climate change simulation data (Murphy et al. 2004), we used averaged multiple model predictions in preference to the results from a single model. These data, provided by China's National Climate Center, were generated using reliability ensemble averaging (Liao 2013; Xu et al. 2010) of the 20 climate models from the World Climate Research Programme's (WCRP's) Coupled Model Intercomparison Project phase 3 (CMIP3) multi-model dataset (Meehl et al. 2007). As recommended by IPCC-SRES (2000) and IPCC-TGICA (2007), we used a range of IPCC-SRES (2000) scenarios covering a variety of assumptions regarding driving forces, selecting scenario A1B, A2 and B1. Prediction of precipitation and temperature time series were based on bilinear interpolation of the original  $1 \times 1^\circ$  baseline GCM data. The predicted monthly data were then downscaled to a daily time-step using the weather generator BCCRCG-WG (Xu et al. 2010). BCCRCG-WG uses first order Markov Chain and two-parameter Gamma distribution for precipitation event simulation, and the non-precipitation variable simulation is based on Fourier series with multi-variable weak stationary process. Previous studies have shown that BCCRCG-WG successfully simulates daily precipitation and non-precipitation variables in China (Li et al. 2013).

### 3.5 Land Cover Change Scenarios

We developed future land cover change scenarios using a combined Cellular automata (CA) - Markov model, which possesses the strengths of both of these modelling approaches (Guan et al. 2011), within IDRISI software (Eastman 2001). The main steps were:

1. The Markov module was used to analyze a pair of land cover distribution maps and output a transition probability matrix, a transition areas matrix, a collection of conditional probability images, and transition suitability image.
2. The standard  $5 \times 5$  contiguity filter was used to generate a spatially explicit contiguity-weighting factor to change the state of cells based on its adjacent cellular state.
3. Five-year loop iterations were used for the CA module to simulate a future land cover distribution map.
4. The land cover map was compared with the actual land cover map to test model accuracy according to Cramer's *V* and Cohen's Kappa statistics (Rees 2008). The steps were repeated until the satisfactory simulation of the land cover distribution was achieved.

### 3.6 Establishing the Relative Contributions of Climate and Land Cover Change Impact on Runoff

The parameters of the SWAT models were calibrated using hydrological data and land cover distribution data from the baseline period to represent runoff characteristics under the condition

of a low level of human disturbance. The calibrated model was then run for the historical impacted period using historical meteorological data from the impacted period. The model was also run for future climate change scenarios, with the assumption of constant land cover distribution as for the baseline period. These model runs isolated the effect of climate change on runoff from that of land cover change. The average annual runoff change as a result of climate change ( $\Delta R_c$ ) was calculated as:

$$\Delta R_c = R_{ic} - R_b \quad (1)$$

where  $R_{ic}$  is the average annual modelled runoff in the impacted period with the impact of climate change, and  $R_b$  is the average annual modelled runoff in the baseline period.

The calibrated model for the historical impacted period was run using historical land cover and historical meteorological data from the impacted period, which simulated the combined impact of climate change and land cover change. For each of the two future land cover change scenarios the model was run for each of the three future climate change scenarios, comprising six scenarios for each catchment. The average annual runoff change as a result of land cover change ( $\Delta R_l$ ) was calculated as:

$$\Delta R_l = R_{icl} - R_{ic} \quad (2)$$

where  $R_{icl}$  is the average annual modelled runoff in the impacted period with the impact of both climate change and land cover change.

The relative contributions of climate change and land cover change to total runoff change, defined as  $\beta_c$  and  $\beta_l$  respectively, were calculated as:

$$\beta_c = \frac{\Delta R_c}{R_b} \times 100\%, \quad \beta_l = \frac{\Delta R_l}{R_b} \times 100\% \quad (3)$$

## 4 Results

### 4.1 Trend and Step Change Analysis for Historical Hydrological Series

The time series of annual observed runoff, precipitation and potential evapotranspiration highlight the relative dryness of the Luan River catchment compared to the upper Han River catchment (Fig. 2). In both catchments the annual precipitation series had no trend, while the annual runoff and potential evapotranspiration series had significant decreasing trends. There were no step changes in either of the precipitation series. Significant step changes in runoff occurred in 1985 in the upper Han River (for CD test only), and in 1979 in the Luan River (for CD, WLR and CUSUM tests). For both study catchments, the baseline periods (1961–1985 for upper Han River and 1960–1979 for Luan River) did not have significant trend in runoff and there was little land cover change over these periods.

### 4.2 Description of Future Climate Change Scenarios

The annual precipitation change series of the climate change scenarios (Fig. 3) had significant trend for scenario A1B in both catchments, and scenario B1 in the upper Han River catchment (Table 1). Although the mean change rate of precipitation was positive for all but one scenario (A2 in the Luan River catchment), the means of annual precipitation were not significantly different to those of the baseline series. In contrast, the annual temperature difference series of

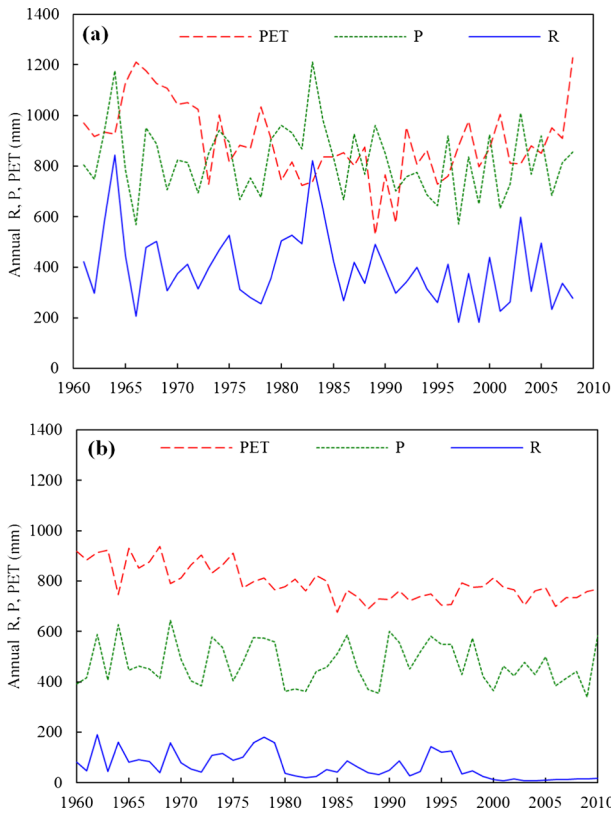


**Fig. 2** Historical annual runoff (*R*), precipitation (*P*) and potential evapotranspiration (*PET*) in (a) upper Han River catchment and (b) Luan River catchment

the climate change scenarios (Fig. 3) had significant increasing trend, and the means of the temperature series were significantly higher than those of the baseline temperature series (Table 1).

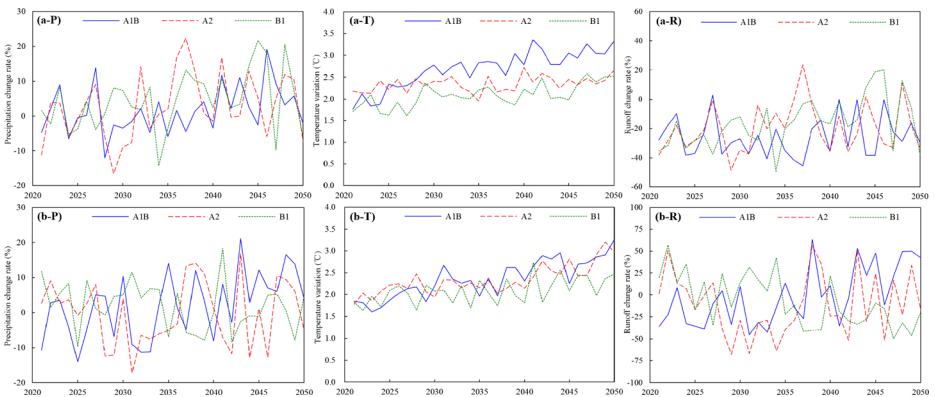


**Fig. 3** Annual precipitation change rate (*P*), temperature variation (*T*), runoff change rate (*R*) relative to baseline for (a) upper Han River catchment and (b) Luan River catchment, under three climate change scenarios



**Table 1** Mann-Kendall (MK) trend test results, and descriptive statistics, for annual precipitation change and temperature difference for three climate change scenarios (over the period 2021–2050), relative to the historical baseline series

Catchment	Scenario	Precipitation change			Temperature difference		
		MK z-test	Slope (%/a)	Mean change rate (%)	MK z-test	Slope (°C/a)	Mean difference (°C)
Upper Han River	A1B	2.00 (*)	0.22	1.63 (ns)	5.50 (**)	0.04	2.69 (**)
	A2	1.43 (ns)	–	2.60 (ns)	2.21 (*)	0.01	2.35 (**)
	B1	2.11 (*)	0.46	4.44 (ns)	3.57 (**)	0.02	2.09 (**)
Luan River	A1B	2.71 (**)	0.52	2.12 (ns)	5.42 (**)	0.04	2.36 (**)
	A2	0.04 (ns)	–	–0.10 (ns)	4.64 (**)	0.03	2.33 (**)
	B1	–1.68 (ns)	–	1.90 (ns)	2.96 (**)	0.02	2.09 (**)

Significance is \*\*= $p < 0.01$ , \*= $p < 0.05$ , *ns* not significant at  $\alpha = 0.05$ ; significance of mean precipitation change rate and mean temperature difference is Student's *t* test of difference of means of climate change precipitation and temperature series and the historical baseline period precipitation and temperature series

#### 4.3 Land Cover Change

Land cover of two catchments mostly comprised forest, woodland, dryland agriculture and grassland (Fig. 4). In the Luan River catchment, between 1980 and 1990 the percentage of forest and woodland increased at the expense of paddy, dryland agriculture, grassland and desert (Fig. 4). Between 1990 and 2000 the land cover reverted to a pattern similar to that of 1980, except for urban land area, which continued to increase. In the upper Han River catchment, the changes in land cover between the three observed years were small, but followed a pattern similar to that observed in the Luan River catchment (Fig. 4). On this basis, we established two future land cover scenarios. One scenario was based on the trend of land cover between 1980 and 1990, which was characterized by conversion of some areas of grassland and dryland agriculture to forest and woodland (G-F). The other scenario was based on the trend of land cover between 1990 and 2000, which was characterized by conversion of some areas of forest and woodland to grassland and dryland agriculture (F-G). The CA-Markov model simulated contrasting future land cover distributions for these two scenarios for 2025, 2035, and 2045, with the change in land cover amplified over time (Fig. 4). The three modelled land cover distributions for 2025, 2035 and 2045 were assigned to represent 10 year long periods in the SWAT model runs of future scenarios (Table 2).

#### 4.4 SWAT Model Calibration and Validation

The calibrated SWAT models predicted monthly runoff series that were close to the observed runoff series, and the models also performed well in the validation period, even though some peaks were over- or under-estimated (Fig. 5). The 95PPU interval was narrow, and most of the observed values were inside the 95PPU, indicating consistency and robustness in model simulation for the calibration and validation periods. Goodness-of-fit tests suggested that performance of the calibrated models was satisfactory for the purpose of predicting runoff for the future climate and land cover change scenarios.



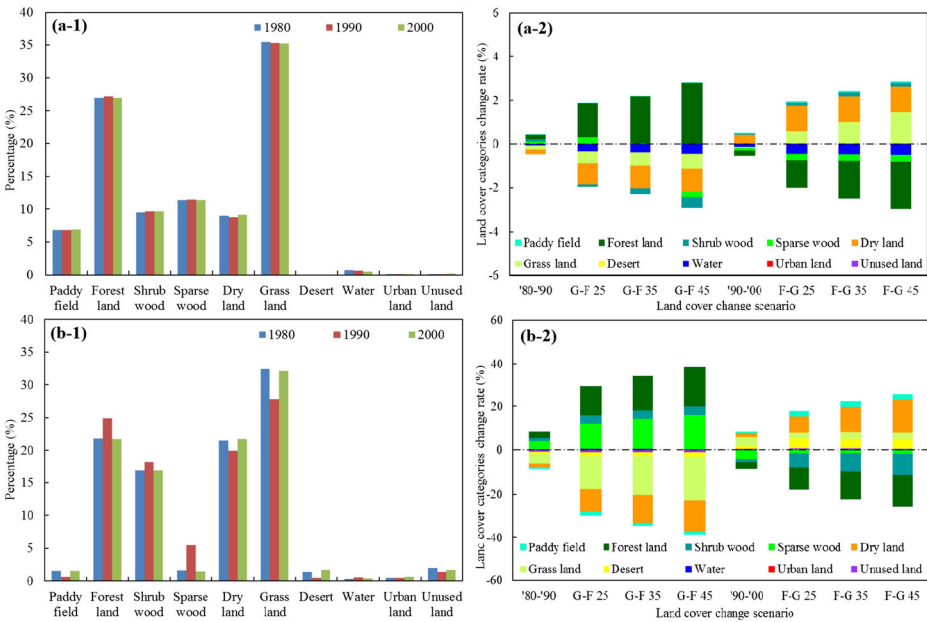


**Fig. 4** Measured land cover change for three history periods (1), land cover categories change rate for two future scenarios (2) for (a) upper Han River catchment and (b) Luan River catchment

4.5 Impacts of Climate and Land Cover Changes on Runoff Over the Historical Period

Over the historical period, annual precipitation in the impacted period was not significantly different to that of the baseline period, but there was a significant difference in mean temperature, annual runoff and runoff coefficient (Table 3). Land cover change was slight in the upper Han River catchment (Fig. 4), so only 2 % of the change in runoff was attributed to this factor (Table 4). Land cover change was more substantial in the Luan River catchment (Fig. 4), but even so, the contribution of climate change to runoff change (15.4 %) was more than four times that of land cover change (3.3 %) (Table 4).

**Table 2** Land cover distributions assumed in the SWAT model for each modelled time period

Conditions		Upper Han River catchment		Luan River catchment	
		Time period	Land cover distribution	Time period	Land cover distribution
Historical	Baseline	1961–1985	1980	1960–1979	1980
	Impacted	1986–1995	1990	1980–1995	1990
		1996–2008	2000	1996–2010	2000
Future	Impacted	2021–2030	2025	2021–2030	2025
		2031–2040	2035	2031–2040	2035
		2041–2050	2045	2041–2050	2045

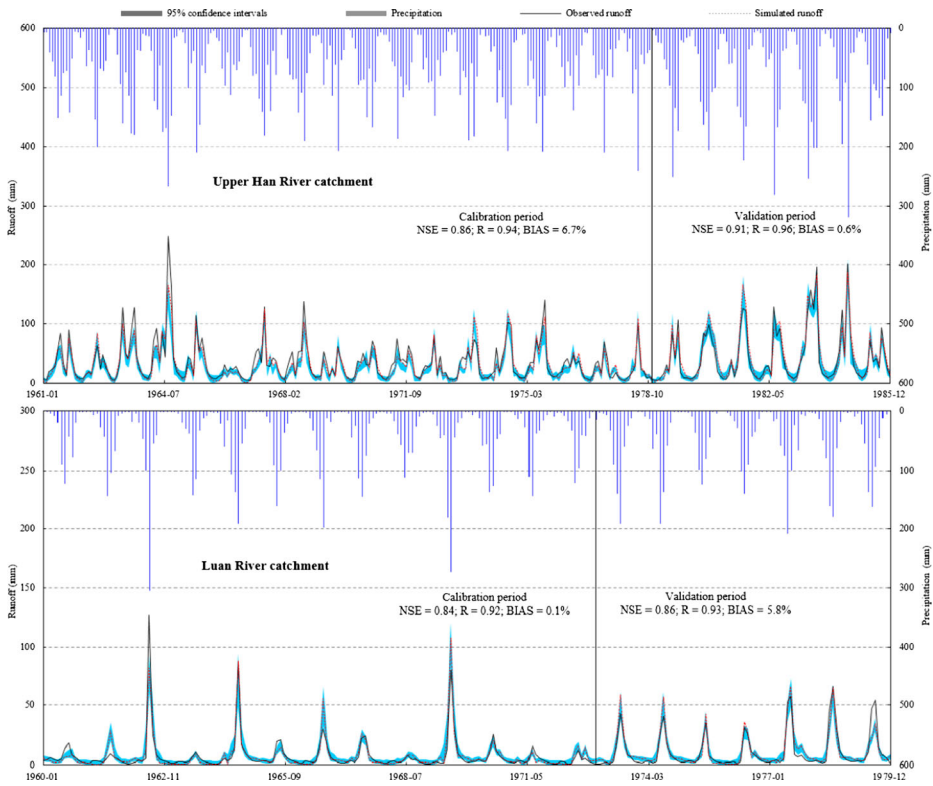


**Fig. 5** Comparison of observed and simulated monthly runoff for calibration and validation periods and the 95 % prediction uncertainty interval of monthly runoff

**Table 3** Comparison of annual mean precipitation, temperature, observed runoff and runoff coefficient for the historical baseline and impacted periods

Catchment	Period	Mean precipitation (mm)	Mean temperature (°C)	Mean runoff (mm)	Mean runoff coefficient
Upper Han River	Baseline period (1961–1985)	854.3	14.46	446.8	0.51
	Historical impacted period (1986–2008)	784.5	14.72	341.2	0.43
	Difference (sig.)	-8 % (ns)	0.26 °C (**)	-24 % (*)	-16 % (**)
Luan River	Baseline period (1960–1979)	491.9	6.59	103.5	0.20
	Historical impacted period (1980–2010)	462.0	7.23	41.2	0.08
	Difference (sig.)	-6 % (ns)	0.64 °C (*)	-60 % (**)	-58 % (**)

Significance of difference in means tested by Student’s *t* test

Significance is \*\*= $p < 0.01$ , \*= $p < 0.05$ , ns=not significant at  $\alpha = 0.05$

**Table 4** Modelled contribution of climate change and land cover change to runoff for the historical impacted period

Catchment	Modelled runoff (mm)			Average annual change in runoff (mm)		Contribution to change in runoff (%)	
	Baseline period	Impacted period with climate change	Impacted period with climate and land cover change	Due to climate change	Due to land cover change	Climate change	Land cover change
	$R_b$	$R_{ic}$	$R_{icl}$	$\Delta R_c$ (Eq. 1)	$\Delta R_l$ (Eq. 2)	$\beta_c$ (Eq. 3)	$\beta_l$ (Eq. 3)
Upper Han River	424.85	384.24	384.17	-40.61	-0.07	-9.56	-0.02
Luan River	106.15	89.83	86.37	-16.32	-3.46	-15.38	-3.26

Negative sign indicates that the impact is decreased runoff

#### 4.6 Impacts of Climate and Land Cover Changes on Runoff Over Future Scenario Periods

Only climate change scenario B1 had a significant trend for runoff in the upper Han River catchment, while scenarios A1B and B1 had a significant trend in the Luan River catchment (Fig. 3, Table 5). Scenario B1 had an increasing trend in the upper Han River catchment, but a decreasing trend in the Luan River catchment (Table 5). Over the entire modelled future period, the average runoff was 5–15 % lower than baseline under the climate change scenarios except for scenario A1B in the Luan River catchment, where the period average runoff was 1 % higher than baseline (Table 5).

Compared to baseline, the F-G scenario had increased runoff, and the G-F scenario had decreased runoff (Fig. 6), which is in agreement with a large body of literature indicating that runoff from grass land cover is higher than that from forest (e.g., Zhang et al. 2001). Of the 12 modelled time series, only four had significant trend (Table 6). This is partly explained by the high inter-annual variability of the data (Fig. 6) and partly because the majority of the land cover change occurred in the early part of the modelled future period, before 2025 (Fig. 4).

#### 4.7 Impacts of Climate Change and Land Cover Change on Mean Annual River Flow

All of the upper Han River climate and land cover change scenarios predicted lower mean annual inflow to Danjiangkou Reservoir compared with the baseline flows over the period

**Table 5** Summary of statistical analysis for annual runoff change rate under three climate change scenarios

Catchment	Scenario	MK z-test	Slope (%/a)	$\beta_c$ (%) (Eq. 3)
Upper Han River	A1B	0.93 (ns)	–	-15.16
	A2	1.57 (ns)	–	-10.34
	B1	3.24 (*)	1.22	-6.50
Luan River	A1B	3.50 (**)	2.52	0.98
	A2	1.14 (ns)	–	-9.15
	B1	-3.28 (*)	-2.22	-4.75

Significance is \*\*= $p < 0.01$ , \*= $p < 0.05$ , ns not significant at  $\alpha = 0.05$

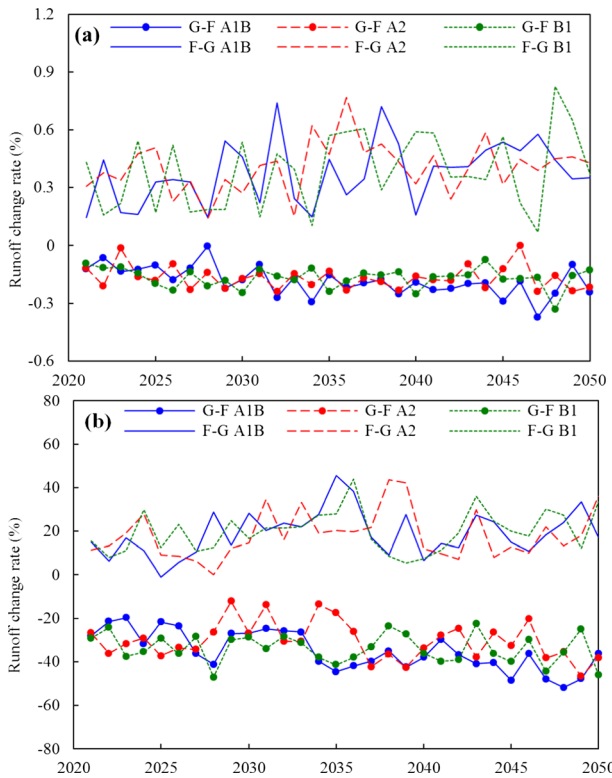


**Fig. 6** Annual runoff change rate for (a) upper Han River catchment, and (b) Luan River catchment under two land cover change scenarios. Change rate is scenario annual runoff relative to mean annual runoff for climate change-only scenarios

1961–1985, with the difference being within 15 %, or  $63.8 \times 10^8 \text{ m}^3$  (Fig. 7). Only small changes in land cover were predicted, and climate and land cover change acting together would be expected to reduce mean annual flow by up to  $64.6 \times 10^8 \text{ m}^3$ . In the Luan River,

**Table 6** Summary of statistical analysis for annual runoff change rate under two land cover change scenarios, for the three climate change scenarios

Catchment	Climate Scenario	Some grassland and dryland agriculture to forest and woodland (scenario G-F)			Some forest and woodland converted to grassland and dryland agriculture (scenario F-G)		
		MK z-test	Slope (%/a)	$\beta_t$ (%) (Eq. 3)	MK z-test	Slope (%/a)	$\beta_t$ (%) (Eq. 3)
Upper Han River	A1B	-3.10 (*)	-0.008	-0.19	2.25 (*)	0.008	0.39
	A2	-0.96 (ns)	-	-0.18	1.21 (ns)	-	0.42
	B1	-0.71 (ns)	-	-0.18	1.53 (ns)	-	0.40
Luan River	A1B	-3.78 (**)	-0.764	-35.09	1.39 (ns)	-	19.03
	A2	-1.36 (*)	-0.241	-30.35	1.11 (ns)	-	18.38
	B1	-1.18 (ns)	-	-33.88	1.50 (ns)	-	19.93

Significance is \*\*= $p < 0.01$ , \*= $p < 0.05$ , ns not significant at  $\alpha = 0.05$

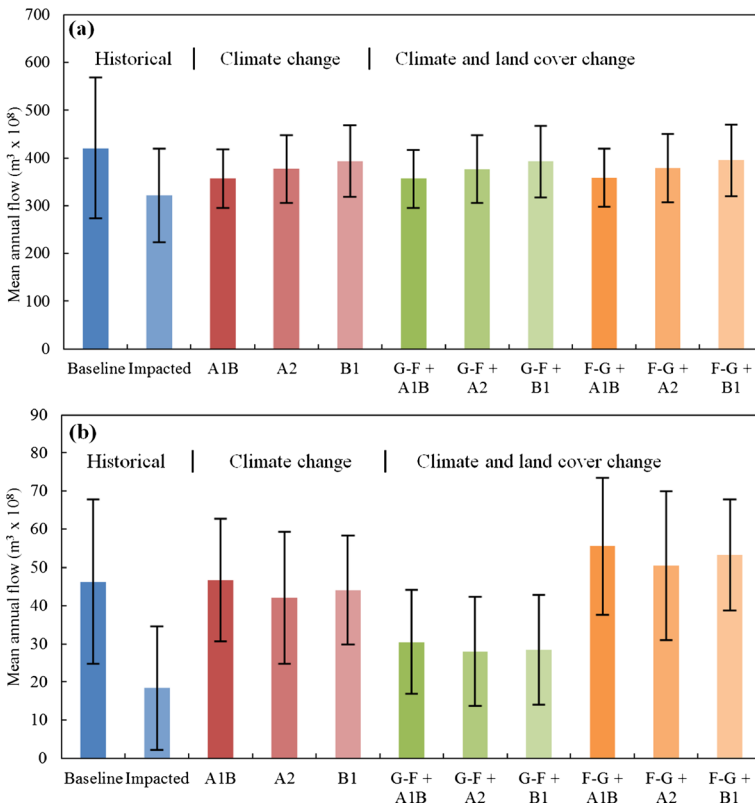


**Fig. 7** Historical and modelled mean annual flow and standard deviation for (a) upper Han River catchment, and (b) Luan River catchment under climate change and land cover change scenarios

climate change alone would be expected to reduce annual river flow by up to 9 %, or  $4.2 \times 10^8 \text{ m}^3$  (Fig. 7). If the historical patterns and rates of land cover change were to continue into the future, then combined with climate change, the change in mean annual river flow relative to baseline flows over the period 1960–1979 could vary from a reduction of up to  $18.3 \times 10^8 \text{ m}^3$  to an increase of up to  $9.3 \times 10^8 \text{ m}^3$  (Fig. 7).

#### 4.8 Historical River Flows and Diversions

In both the upper Han River and Luan River, of all the time series that were evaluated, the one with the lowest river flow was the historical impacted period (Fig. 7). In the upper Han River, the mean annual flow for the impacted period 1986–2008 was  $99.4 \times 10^8 \text{ m}^3$ , or 24 %, lower than that of the baseline period. In the Luan River, the mean annual flow for the impacted period 1980–2010 was  $27.8 \times 10^8 \text{ m}^3$ , or 60 %, lower than that of the baseline period (Fig. 7). The models predicted the impact of climate change and land cover change on runoff, but some of the observed change in historical runoff could have been associated with increasing diversion of water from the rivers.

In the upper Han River, over the impacted historical period, the annual flows modelled on the basis of land cover change and climate change were similar to the historical annual flows (not illustrated in this paper), which is not surprising considering the low levels of diversions in

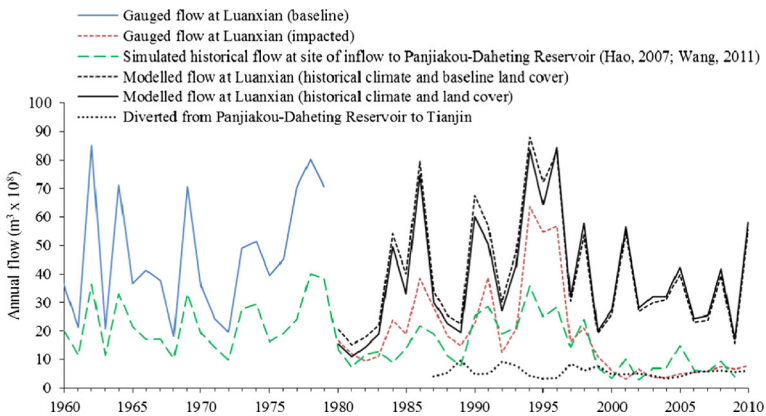


**Fig. 8** Historical gauged and modelled mean annual flows for Luan River

the upper Han River catchment. In contrast, in the Luan River, the historical flows in the impacted period were much lower than the flows modelled on the basis of land cover change and climate change, especially after 1998 (Fig. 8).

The relationship between historical flows at the site of inflow to the Panjiakou-Daheting Reservoir system (operational from 1981) and a statistically significant change point occurred in the time series of flows at the site of inflow to the reservoir in 1998 (Fig. 8). Before the change point in flows at Luanxian in 1979, annual flow at the site of inflow to the reservoir averaged 50 % of the annual flow at Luanxian and was relatively consistent (Fig. 8). After 1979, the relationship changed dramatically (Fig. 8), with annual reservoir inflow exceeding flow downstream at Luanxian in about 40 % of years. Diversions from the reservoir from 1981 onwards only partially explain this observation. The Annual average diversions from the reservoir to Tianjin over the period 1987–2010 was  $5.70 \times 10^8 \text{ m}^3$  (Fig. 8), which accounted for about 60 % of the originally planned maximum annual allocation, suggesting that flows in the river were lower than had been anticipated in the planning process. Under average hydrological conditions this volume of diversion would allow outflows from the reservoir to the river downstream, but in 1989, and in most years from 1998 onwards, most or all of the inflow to the reservoir system was diverted to Tianjin (Fig. 8).

Until 1999, annual diversions to Tianjin were negatively correlated with both reservoir system inflows (Pearson  $r = -0.655$ ,  $p < 0.05$  two tailed probability) and flows at Luanxian (Pearson  $r = -0.776$ ,  $p < 0.01$  two tailed probability). However, from 2000 onwards, annual diversions to Tianjin were positively correlated with flows at Luanxian (Pearson  $r = 0.749$ ,  $p < 0.01$  two tailed probability) and uncorrelated with inflows to the reservoir system. After 1998, runoff in the Luan River fell dramatically and did not recover (Fig. 8). Post-1998, mean annual inflow to the reservoir fell to 35 % of the mean annual flow over the prior period 1960–1998. At Luanxian the mean annual post-1998 flow was only 17 % of the 1960–1998 mean, and 30 % if diversions to Tianjin were added to the river flows. Water use within the Luan River catchment grew from  $1 \times 10^8 \text{ m}^3$  in the 1950s and 1960s to  $6 \times 10^8 \text{ m}^3$  in 2002 (Li and Feng 2007). Although a significant volume, this, together with diversions, climate change and land cover change, is insufficient to fully explain the decline in river runoff after 1998. In the Hai River basin, irrigation has become increasingly reliant on groundwater pumping (Yang and Tian 2009), which could explain a significant proportion of the decline in river flows in the Luan River, as recognized elsewhere (e.g., Peisert and Sternfeld 2005).

#### 4.9 Uncertainty in Results

Regardless of the methodology used, there is uncertainty in climate prediction (Foley 2010), land cover change prediction (Lambin et al. 2001) and SWAT model (Al-Mukhtar et al. 2014). One source of uncertainty in prediction of runoff from precipitation was the necessary assumption that the calibrated model parameters would remain valid in the impacted periods (Merz et al. 2011). We used well-known existing data sets, and applied standard modelling methods that aim to minimize uncertainty, so the uncertainty associated with our results would be similar to that of other studies reported in the literature.

### 5 Implications of Runoff Changes for River Health

The SNWTP will need to balance human and environmental demands for water in both the upper Han River water supply zone and the Hai River water demand zone. The upper Han River could experience an average annual climate change-related decline in water resources availability of up to 15 %, or  $64.6 \times 10^8 \text{ m}^3$  (Fig. 7), which represents half of the intended annual transfer volume from the Danjiangkou Reservoir. The Han River has already experienced significant hydrological, water temperature change and significant water quality concerns since operation of Danjiangkou Reservoir and other regulating structure, with implications for the health of fish communities (Shi and Huang 2009; Zhang 2009; Li et al. 2013). Over the baseline period 1961–1985, the upper Han River contributed an average of 4.7 % of the annual discharge of the Yangtze River at the most downstream gauge (Datong), so management of Han River flows also has implications for environmental flow requirements of the lower Yangtze River.

In every year since 2000, the annual flow of the Luan River at Luanxian has been less than the ‘suitable ecological water demand’ of  $8.2 \times 10^8 \text{ m}^3$  suggested by Yan et al. (2012), a minimum threshold thought to be suitable for maintenance of river health. It is worth noting that for this river Wang et al. (2009) estimated a ‘medium’ annual environmental water requirement of  $8.9 \times 10^8 \text{ m}^3$  and an ‘ideal’ of  $16.3 \times 10^8 \text{ m}^3$ . Prior to 2000, the annual flow exceeded the ‘medium’ level in every year, and the ‘ideal’ level in 87 % of years (Fig. 8), so, while higher than the ‘suitable ecological water demand’, these cannot be considered particularly generous recommendations. Consider also that for the Hai, Huai and Huang River basins, it has been estimated that 72 % more water is required for maintenance of healthy ecosystems compared to that required just to prevent further decline (Yang and Zehnder 2005).

Our analysis suggests that in the Luan River, while future climate change could reduce water availability relative to baseline conditions by up to 9 %, or  $4.2 \times 10^8 \text{ m}^3$ , land cover change acting with climate change could reduce it by up to 40 %, or  $18.3 \times 10^8 \text{ m}^3$  (Fig. 7). Although these predicted flow declines are concerning, they are still smaller than the flow reduction that has already happened due to extraction of water directly from rivers and likely extraction from river-connected groundwater. This means that even if the SNWTP allows for decommissioning of the Tianjin and Tangshan diversions from the Luan River, restoration of river health is unlikely without some form of flow supplementation or reduction in local abstractions.

### 6 Conclusions

The main conclusion of this study are:



- (1) Future climate change to 2050 is likely to significantly increase temperature in the catchments, but not precipitation. This change will cause an average reduction in runoff of up to 15 % in the upper Han River and up to 9 % in the Luan River catchment. A land cover change scenario involving increased forest cover would reduce runoff by up to 0.19 % in the upper Han River and up to 35 % in the Luan River. A scenario involving increased grass cover would increase runoff by up to 0.42 % in the upper Han River and up to 20 % in the Luan River.
- (2) Future climate change and land cover change acting together to 2050 could decrease mean annual inflows to the Danjiangkou Reservoir of the upper Han River catchment by up to  $63.8 \times 10^8 \text{ m}^3$ . In the Luan River, future climate and land cover changes could decrease mean annual river flows by up to  $18.3 \times 10^8 \text{ m}^3$  or increase flows by up to  $9.3 \times 10^8 \text{ m}^3$ , depending on the direction of land cover change.
- (3) In the Luan River, the predicted future impacts on runoff are less than the flow reduction that has already occurred since 1998, due to extraction of water directly from rivers and from river-connected groundwater. Improvements in river health could be an outcome if the Tianjin and Tangshan diversions from the Luan River were decommissioned, but supplementary actions might also be required.
- (4) Altered hydrology and pollution have degraded the health of the Han River downstream of the Danjiangkou Reservoir. Future declines in inflows to the reservoir together with diversions via the SNWTP will increase the hydrological stress in the river downstream, and potentially in the Yangtze River.
- (5) Climate change and land cover change are likely to impact future water resources availability, but we found that current direct human interference in the water cycle, in the form of surface water and groundwater abstraction, was of more significant concern to the availability of water for sharing among a range of human uses and maintenance of river health.

**Acknowledgments** This study was supported by the State Key Program of National Natural Science of China (NO. 51339004) and the National Natural Science Foundation of China (NO. 51279139 and NO. 51279139). The contribution of CJG was supported by the High-End Foreign Expert Recruitment Programme, administered by the State Administration of Foreign Experts Affairs, Central People's Government of P.R. China. We acknowledge the modeling groups, the Program for Climate Model Diagnosis and Intercomparison (PCMDI) and the WCRP's Working Group on Coupled Modelling (WGCM) for their roles in making available the WCRP CMIP3 multi-model dataset. Support of this dataset is provided by the Office of Science, U.S. Department of Energy.

## References

- Abbaspour KC (2007) User manual for SWAT-CUP SWAT calibration and uncertainty analysis programs. Swiss Federal Institute of Aquatic Science and Technology (Eawag), Dübendorf
- Al-Mukhtar M, Dunger V, Merkel B (2014) Assessing the impacts of climate change on hydrology of the upper reach of the spree river: Germany. *Water Resour Manag* 28:2731–2749
- Berkoff J (2003) China: the south–north water transfer project—is it justified? *Water Policy* 5:1–28
- Cao W, Bowden WB, Davie T et al (2009) Modelling impacts of land cover change on critical water resources in the Motueka River catchment, New Zealand. *Water Resour Manag* 23(1):137–151
- Chiew FHS, McMahon TAM (1993) Detection of trend or change in annual flow of Australian rivers. *Int J Climatol* 13:643–653
- Chiew FHS, Siriwardena L (2005) Trend, trend/change detection software, user guide. CRC for Catchment Hydrology, University of Melbourne, Melbourne
- Eastman JR (2001) IDRISI 32 release 2, guide to GIS and image processing volumes 1 and 2. Clark Labs, Clark University, Worcester

- Foley AM (2010) Uncertainty in regional climate modelling: a review. *Prog Phys Geog* 34(5):647–670
- Gassman PW, Reyes MR, Green CH et al (2007) The soil and water assessment tool historical development, applications, and future research directions. *Trans ASABE* 50(4):1211–1250
- Guan DJ, Li HF, Inohae T et al (2011) Modeling urban land use change by the integration of cellular automaton and Markov model. *Ecol Model* 222(20–22):3761–3772
- Hao J (2007) Research on causation and countermeasure of incoming runoff decrease for Panjiakou Reservoir. *Water Resour Hydropower En* 38(16):8–11 (in Chinese)
- IPCC-SRES (2000) Special report on emissions scenarios. In: Nakićenović N, Swart R (eds) A special report of working group III of the intergovernmental panel on climate change. Cambridge University Press, Cambridge
- IPCC-TGICA (2007) General guidelines on the use of scenario data for climate impact and adaptation assessment. Version 2. Prepared by TR Carter on behalf of the Intergovernmental Panel on Climate Change, Task Group on Data and Scenario Support for Impact and Climate Assessment, 66 pp
- Lambin EF, Turner BL, Geist HJ et al (2001) The causes of land-use and land-cover change: moving beyond the myths. *Global Environmental Change-Human and Policy Dimensions* 11(4):261–269
- Li JZ, Feng P (2007) Runoff variations in the Luanhe River Basin during 1952–2002. *J Geogr Sci* 17(3):339–350. doi:10.1007/s11442-007-0339-8
- Li BS, Zhou PJ, Wang XU et al (2013) Opportunities and eco-environmental influence of cascade hydropower development and water diversion projects in Hanjiang River Basin. *J Geol Soc India* 82:692–700
- Liao YM (2013) Change of parameters of BCCRCG-WG for daily non-precipitation variables in China 1951–1978 and 1979–2007. *J Geogr Sci* 23(4):579–594
- Meehl GA, Covey C, Delworth T et al (2007) The WCRP CMIP3 multi-model dataset: a new era in climate change research. *Bulletin of the American Meteorological Society* 88:1383–1394. doi:10.1175/BAMS-88-9-1383
- Merz R, Parajka J, Blöschl G (2011) Time stability of catchment model parameters: implications for climate impact analyses. *Water Resour Res* 47(2), W02531. doi:10.1029/2010WR009505
- Murphy JM, Sexton DM, Barnett DN et al (2004) Quantification of modelling uncertainties in a large ensemble of climate change simulations. *Nature* 430(7001):768–772
- Narsimlu B, Gosain AK, Chahar BR (2013) Assessment of future climate change impacts on water resources of upper sind river basin, India using SWAT model. *Water Resour Manag* 27(10):3647–3662
- Peisert C, Sternfeld E (2005) Quenching Beijing's thirst: the need for integrated management for the endangered Miyun Reservoir. *China Environment Series* 7:33–46
- Rees WG (2008) Comparing the spatial content of thematic maps. *Int J Remote Sens* 29(13):3833–3844
- Sen PK (1968) Estimates of the regression coefficient based on Kendall's tau. *J Am Stat Assoc* 39:1379–1389
- Shi FF, Huang W (2009) Ecological impacts of the Danjiangkou Reservoir on the middle and lower reaches of the Han River. *Resources and Environment in the Yangtze Basin* 18(10):954–958 (in Chinese)
- Shi P, Ma X, Hou Y et al (2013) Effects of land-use and climate change on hydrological processes in the Upstream of Huai River, China. *Water Resour Manag* 27(5):1263–1278
- Tianjin Water Supply Bureau (2000–2010) Water resources bulletin of Tianjin, for years 2000 to 2010. Tianjin Water Supply Bureau, Tianjin City
- Wang SM (2011) The impact of inter-basin water supply on sustainability of social and economic development in Tianjin and Tangshan—a case study of the Luan River Diversion project. In Proceedings, Conference of Chinese Environmental Science Institute, November, Vol. 1: 286–291 (in Chinese)
- Wang W, Yang XH, Wang YT (2009) Ecological water requirements in the lower reaches of the Luanhe River Basin. *Adv Water Sci* 20:560–565 (in Chinese)
- Xia J, Zhang L, Liu C et al (2007) Towards better water security in North China. *Water Resour Manag* 21(1):233–247
- Xu Y, Gao XJ, Giorgi F (2010) Upgrades to the reliability ensemble averaging method for producing probabilistic climate-change projections. *Clim Res* 41(1):61–81
- Yan DH, Wang G, Wang H et al (2012) Assessing ecological land use and water demand of river systems: a case study in Luanhe River, North China. *Hydrol Earth Syst Sc* 16:2469–2483. doi:10.5194/hess-16-2469-2012
- Yang YH, Tian F (2009) Abrupt change of runoff and its major driving factors in Haihe River Catchment, China. *J Hydrol* 374(3–4):373–383
- Yang H, Zehnder AJB (2005) The south–north water transfer project in China. *Water Int* 30(3):339–349. doi:10.1080/02508060508691874
- Zhang QF (2009) The south-to-north water transfer project of China: environmental implications and monitoring strategy. *J Am Water Resour As* 45(5):1238–1247
- Zhang Z, Dawes WR, Walker GR (2001) Response of mean annual evapotranspiration to vegetation changes at catchment scale. *Water Resour Res* 37(3):701–708
- Zhang C, Ren J, Gao X et al (2008) Study on two-part water price model for water diversion project from Luanhe River to Tianjin. *China Water Wastewater* 24(4):72–75 (in Chinese)
- Zhang LP, Qin LL, Yang Z et al (2012) Climate change impacts on hydrological processes in the water source area of the middle route of the south-to-north water diversion project. *Water Int* 37(5S):564–584